JOURNAL OF GEOPHYSICAL RESEARCH, VOL. 97, NO. D18, PAGES 20,717–20,729, DECEMBER 20, 1992

Photochemical Aerosol Formation From α-Pinene- and β-Pinene

SHOU-HUA ZHANG, MARTHA SHAW, JOHN H. SEINFELD, AND RICHARD C. FLAGAN

Department of Chemical Engineering, California Institute of Technology, Pasadena, California

Aerosol formation from α-pinene and β-pinene was studied in a series of outdoor smog chamber experiments. Since a previous study focused on β-pinene (Pandis et al., 1991), more attention was given here to α-pinene. The initial hydrocarbon and NO_x concentrations ranged from 37 to 582 ppb and 31 to 380 ppb, respectively. The aerosol carbon yield, the fraction of the carbon initially present that is converted to aerosol, varied from 0 to 5.3% for α-pinene, depending on the initial hydrocarbon-to-NO_x ratio. Dual-bag experiments demonstrate that α-pinene is more rapidly photooxidized, and produces higher yields of both aerosol and ozone in a given period of time than β-pinene, although given sufficient time β-pinene can produce equivalent aerosol yields. Although aerosol formation solely from isoprene photooxidation was found in a previous study to be negligible under ambient conditions, the addition of isoprene to the α-pinene/NO_x system leads to an increased aerosol yield through the enhanced photochemical activity generated.

INTRODUCTION

Understanding the degradation pathways of biogenic hydrocarbons represents an important current problem in atmospheric chemistry. Trees are the principal emitters of such hydrocarbons, with isoprene and α– and β–pinene being the primary species emitted [*Dimitriades*, 1981]. *Lamb et al.* [1987] developed a national inventory of biogenic hydrocarbon emissions by combining emission rate data from various field studies, emission algorithms developed in laboratory studies, biomass density data, and land use and temperature data. They concluded that the emissions are distributed between deciduous and coniferous vegetation, with agricultural crops responsible for less than 3% of the total emissions. Total emissions from coniferous trees were calculated at 21.7 Mt annually, with emissions from deciduous forests at 8.0 Mt. Total emissions rates of isoprene from deciduous forests and α–pinene from deciduous and coniferous forests are estimated as 4.9 and 6.6 Mt annually. The bulk of the remaining emissions is due to other monoterpenes, with β–pinene being the most significant contributor. More than half of the biogenic hydrocarbon emissions are estimated to occur in the summer, and approximately half are estimated to arise in the southeast and southwest United States.

Although the aerosol-forming potential of monoterpenes has been recognized since 1960 [*Went*, 1960], few quantitative data exist under ambient conditions. The fraction of a hydrocarbon that is converted to aerosol upon photooxidation can be expressed on a mass or carbon concentration basis. Available aerosol yield data for the monoterpenes vary widely and have been found to depend strongly on experimental conditions. *Hull* [1981] and *Kamens et al.* [1981] reported aerosol yields for α-pinene on a mass basis of 51% and 25 to 90%, respectively. Also for α-pinene, *Hooker et al.* [1985] obtained aerosol yields on a carbon basis of 38 to 68%. *Hatakeyama et al.* [1989] studied the reactions of α- and β-pinene with O_3 and OH, reporting aerosol carbon yields of 18.3% and 13.8% for the O_3 reactions and 56% and 44% for the OH reactions. In further work, *Hatakeyama et al.* [1991] found that NO suppressed the aerosol carbon yield for both α- and β-pinene.

Pandis et al. [1991] showed that isoprene is not a significant aerosol precursor under ambient conditions, with a maximum aerosol yield less than 0.8%, even under high concentration conditions. β-pinene photooxidation resulted in aerosol yields between 0.1% to 8%, depending on conditions of the mixture. Aerosol formation was observed for β-pinene concentrations as low as 20 ppb (the minimum concentration studied). The aerosol yield was shown to be strongly dependent on the initial hydrocarbon-to-NO_x concentration ratio. At low ratios of initial β-pinene to NO_x concentrations ($[HC]_o/[NO_x]_o<5$), the aerosol yield is small. The maximum aerosol yield occurred at a ratio of initial concentrations of $[HC]_o/[NO_x]_o$= 10 - 15 ppbC/ppb. Upon increasing this ratio, the aerosol yield again decreased. This observation implies a dual role for NO_x in the formation of aerosol, and also indicates that for olefins for which O_3, OH, and NO_3 are all important oxidants, a single value for aerosol yield is not sufficient to describe this complex behavior. The vapor pressure of the aerosol produced from the photooxidation of β-pinene was estimated to be 37 ± 24 ppt at 304 K based on tandem differential mobility analyzer measurements.

If the reaction mechanism for the photochemical oxidation of each atmospheric hydrocarbon was exactly known, the products could be quantified for each compound, and the amount of aerosol formed per amount of hydrocarbon reacted in any NO_x/oxidant setting could be calculated as long as the vapor pressures of the compounds were known. There have been attempts to model reaction yields of condensable products [*Pandis et al.*, 1991], but direct calculation of secondary aerosol formation potential is uncertain at best, exacerbated by the dearth of kinetic and mechanistic data on entire classes of species. The starting point for determining the aerosol-forming

Paper number 92JD02156
0148-0227/92/92JD-02156$05.00

potential of ambient hydrocarbons is carefully designed experiments in which both gas- and aerosol-phase behavior is accurately measured.

The principal goal of the present study is to evaluate the aerosol-forming potential of α- and β-pinene. Since β-pinene has already been studied by *Pandis et al.* [1991], somewhat more emphasis is placed here on α-pinene. We are particularly interested in the comparative aerosol forming potential of α- and β-pinene and the effect of the initial hydrocarbon-to-NO_x ratio on aerosol formation.

EXPERIMENTAL DESCRIPTION

The Caltech outdoor smog chamber is illustrated in Figure 1, and is similar to that described by *Pandis et al.* [1991]. The smog chamber, constructed by heat-sealing Teflon film, has a volume of approximately 60 m^3. Prior to the beginning of experiments, the tarpaulin covered Teflon chamber was filled with purified air. The purified air was prepared by passing compressed air through three packed beds containing, in turn, silica gel for the removal of moisture, Purafil for the removal of NO_x (Purafil Inc.), Drierite with 13X molecular sieves (Union Carbide), and activated charcoal for the removal of hydrocarbons. The purified air was then passed through a total particle filter. The procedure of injecting gas-phase reactants into the chamber took about 1-2 hours. The biogenic hydrocarbon (Aldrich) was injected with a microsyringe into a glass bulb which was gently heated to evaporate the hydrocabon into an air stream flowing to the chamber. NO and NO_2 were then injected using certified cylinders (Scott-Marrin Inc.). For selected experiments, ammonium sulfate seed particles were injected into the chamber. The seed particles were produced by drying droplets of an aqueous ammonium sulfate solution generated with a constant rate atomizer [*Liu and Lee*, 1975]. The particles passed through a diffusion dryer and a ^{85}Kr neutralizer before entering the chamber.

In the dual-chamber experiments, all of the reactants except one, for example the hydrocarbon, were added to the full chamber and allowed to mix. Then the chamber was divided, and the remaining ingredient was injected accordingly. In this way, the aerosol formation potential of two different hydrocarbons or different concentrations of the same hydrocarbon could be compared at otherwise identical conditions. When the reactants were well mixed and their concentrations became stable, the chamber was uncovered and exposed to sunlight.

The aerosol instrumentation included two differential mobility analyzers (DMA, TSI model 3071) and two condensation nucleus counters (CNC, TSI model 3760) acting as particle detectors. These DMAs and CNCs were controlled by a PC-AT working as a scanning electrical mobility spectrometer (SEMS) [*Wang and Flagan*, 1990] which generated a complete size distribution, 100 data points, for the diameter range of 0.01-0.2 μm in 30 s. For the measurement of particles in the 0.12-5 μm diameter range, a Royco model 226 optical particle counter was used. Both the SEMS and the optical particle counter (OPC) were calibrated with known size polystyrene latex (PSL) particles (Duke Science Inc.). PSL diameters of 0.144, 0.350, 0.509, 0.721 and 0.913 μm were chosen to calibrate the OPC. Monodisperse PSL particles were generated from a constant rate stainless steel atomizer [*Liu and Lee*, 1975] and a diffusion dryer to remove water vapor. The monodisperse PSL particles were used with the OPC to produce the calibration data sets. Subsequently a matrix inversion algorithm was used to invert the experimental OPC data to obtain the particle size distribution.

The total count accuracy for the OPC should be within ±10%, provided the number concentration is less than 1500 cm^{-3} [*HIAC/Royco*, 1982]. When the number concentration exceeded 1500 cm^{-3}, a dilution system was used. The differential mobility analyzer has an accuracy of 2% [*TSI Model 3071 Instruction Manual*, 1983]. With a standard

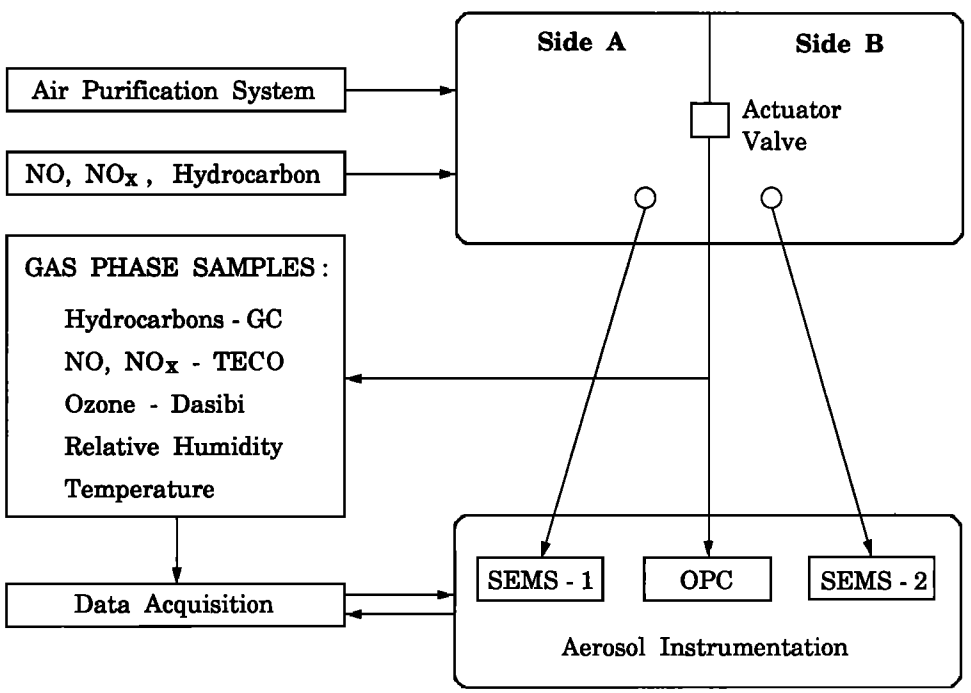

Fig. 1. Outdoor smog chamber facility.

deviation of the PSL particle size of 2.5%, it is reasonable to estimate a size precision of ± 4.5% for particles smaller than 0.2 μm. Copper tubes were used for aerosol sampling to minimize wall losses. The fractional particle losses in the sampling lines from the smog chamber to the instruments were estimated to be less than 2% [*Pandis et al., 199*].

Ozone concentrations were determined with a Dasibi model 1008-PC nondispersive ultraviolet ozone analyzer which was calibrated by Dasibi Environmental Corp. (Glendale, California), and NO and NO_x concentrations were obtained by a Thermo Environmental model 42 chemiluminescent analyzer. The gas-phase concentrations of isoprene, α-pinene, and β-pinene were obtained by gas chromatography (Hewlett-Packard model 5890 equipped with a capillary column and a flame ionization detector). UV solar radiation (Eppley Laboratory pyranometer, model 8-48), chamber temperature and relative humidity were also measured.

In selected experiments, bulk aerosol samples were collected on quartz filters and subsequently analyzed by gas chromatography-mass spectrometry (GC-MS). An eight-stage low pressure impactor [*Hering et al.*, 1978, 1979] was also used to obtain samples for chemical analysis. The aerosol deposits on each stage were examined by Fourier Transform Infrared (FTIR) spectroscopy [*Paulson et al.*, 1990].

The SEMS data were inverted to give the aerosol number size distributions, in the range of 0.01-0.20 μm, and then integrated to give the total number and volume concentrations of the aerosol as functions of time. The raw data from the OPC were inverted with the matrix inversion algorithm to generate the size distributions and number and volume concentrations of the particles larger than 0.12 μm. Combining the inverted data from the SEMS and the OPC, the size distribution, the number concentration, $N(t)$, and volume concentration, $V(t)$, of the aerosol in the entire size range were obtained. The average particle size achieved in the experiments conducted was between 0.07 and 0.18 μm which was in the SEMS measurement range. Therefore, we can assume that the precision of the total measurements is close to that of the SEMS.

Aerosol Volume and Carbon Yield

The aerosol yield from photooxidation of a hydrocarbon can be expressed in several ways. The aerosol volume concentration, $V(t)$, $\mu m^3\ cm^{-3}$, can be used directly to calculate the aerosol volume yield per unit concentration of primary hydrocarbon, $Y(t)$, $\mu m^3\ cm^{-3}\ ppm^{-1}$, as follows,

$$Y(t) = V(t) \Big/ \{[HC]_o - [HC(t)]\} \quad (1)$$

where $[HC]_o$ is the initial concentration of hydrocarbon, and $[HC(t)]$ is the hydrocarbon concentration at reaction time t, expressed in units of ppm. Note that all experiments reported here were carried out with relative humidities, RH, less than 10%. Thus, it can be assumed that the water content of the aerosol was negligible and that the entire aerosol volume was secondary organic product.

The fraction of a particular hydrocarbon that is converted to aerosol can also be expressed on a mass or carbon concentration basis. *Izumi et al.* [1988, 1990] measured the aerosol generated from photooxidation of various hydrocarbons, and correlated the mass concentration of aerosol organic carbon, $[AOC(t)]$ expressed as pg C cm^{-3}, to aerosol volume concentration, $V(t)$ expressed as $\mu m^3\ cm^{-3}$, as

$$[AOC(t)] = C\ V(t) \quad (2)$$

where $C = 0.49 \pm 0.02$, pg C μm^{-3}, represents the aerosol carbon density which was found to be largely independent of the particular hydrocarbon. In the absence of detailed information on the molecular composition and density of the aerosol generated in the present study, equation (2) allows one to relate mass and volume measures of organic aerosol yield.

The dimensionless aerosol carbon yield, Y_c, the fraction of the carbon initially present that is converted to aerosol, can then be obtained from equations (1) and (2) as

$$Y_c = \frac{[AOC(t)]}{f_c\{[HC]_o - [HC(t)]\}} \quad (3)$$

where f_c is a constant to convert hydrocarbon concentration, in ppm, into carbon mass concentration, in pg C cm^{-3}. For α- or β-pinene at 1 atm and 298 K, $f_c = 4908$ (pg C $cm^{-3}\ ppm^{-1}$, or $\mu g\ C\ m^{-3}\ ppm^{-1}$).

Aerosol Formation From the Photooxidation of α-Pinene With NO_x

The initial conditions and key experimental observations for the outdoor smog chamber experiments conducted are summarized in Table 1. Experiments 1S to 13S are single-chamber runs and 14D to 24D were carried out under dual-chamber conditions. The initial hydrocarbon concentrations ranged from 37 to 580 ppb, while the initial NO_x concentrations ranged from 31 to 380 ppb. No nucleation or particle growth was observed in experiments 1S to 4S, and only minor growth was seen in experiment 5S. The aerosol yields of these five runs were virtually zero. In contrast, both nucleation and condensational growth, accompanied by relatively high aerosol yields, were observed in experiments 6S to 13S. It was found that the initial NO and NO_x concentrations influenced the observed aerosol formation and yield.

A number of dual-chamber experiments were carried out under identical conditions of temperature, RH, and solar irradiation. Experiment 19D, which had a medium aerosol yield, typifies α-pinene/NO_x photooxidation and associated aerosol formation. The initial concentrations of NO and NO_x were the same on each side of the chamber, 9.0 and 36.5 ppb, respectively. No seed particles were added. The concentrations of α-pinene were 144 ppb and 57 ppb, and the initial concentration ratios, $[HC]_o/[NO_x]_o$, were 39.4 and 15.6 ppb C/ppb for sides A and B, respectively.

The concentrations of ozone at the beginning of the experiments ranged from 0 to 15 ppb. In most experiments, ozone concentrations increased slowly at the beginning as NO was converted to NO_2, and increased rapidly as the NO concentration approached zero. Ozone reacts with the hydrocarbons studied, so a maximum ozone concentration was frequently observed.

The aerosol evolution on sides A and B in experiment 19D is shown in Figure 2. Nucleation occurred on side A at 50 min, at which time approximately 35 ppb of α-pinene had reacted. In the next 10 min., the aerosol number concentration N increased rapidly, from almost zero to more than 2000 cm^{-3}. Subsequently, the rate of new particle formation slowed as condensation ensued. The average particle size was approximately 0.074 μm at the onset of nucleation. Condensation was evidenced approximately 10 min later than the inception of nucleation. The aerosol number concentration N reached its maximum of 3700 cm^{-3} at 100 min and then decreased gradually due to deposition on the walls of the chamber. The average particle size approached 0.16 μm at 100

TABLE 1. Summary of Initial Conditions and Results Observed

Run	Hydrocarbon	Initial Concentrations HC, ppb	NO, ppb	NO_x, ppb	[HC]/[NO_x] ppb C/ppb	Seeds, cm^{-3}	Ozone, Maximum Time, min	ppb	V_{max} Time, min	V_{max} $\mu m^3\ cm^{-3}$	Y, $\mu m^3\ cm^{-3}\ ppm^{-1}$	Y_c, %
1-S	α-pinene	120.0	355.0	380.0	3.2	250		50		0.00	0.0	0.00
2-S	α-pinene	89.0	23.5	75.0	11.8	195				0.11	4.0	0.04
3-S	α-pinene	62.2	70.0	170.0	3.7	180	275	105		0.04	0.7	0.01
4-S	α-pinene	64.6	24.0	160.0	4.0	960		80		0.30	5.4	0.05
5-S	α-pinene	188.0	170.0	270.0	7.0	800		47	160	1.19	8.1	0.08
6-S	α-pinene	171.6	80.0	120.0	14.3				165	24.7	145	1.44
7-S	α-pinene	401.2	153.0	212.0	18.9	1000			140	89.3	228	2.28
8-S	α-pinene	257.0	26.2	153.0	16.8	450			75	76.1	303	3.03
9-S	α-pinene	273.0	50.0	106.0	25.8	600			100	63.4	232	2.32
10-S	α-pinene	582.0	19.5	58.0	100.4	2400			125	97.1	252	2.51
11-S	α-pinene	515.0	78.0	92.0	56.0		50	71.6	130	236	534	5.33
12-S	α-pinene	370.0	12.0	35.8	103.4	400	40	58	75	150	995	9.93
	and isoprene	613.3										
13-S	α-pinene	157.5	6.8	31.0	50.8	340	40	45	95	51.4	514	5.13
14-D	α-pinene	60.0	32.4	39.0	15.9	no	115	59	170	0.16	2.7	0.03
	α-pinene	37.5	32.4	39.0	9.6	no	100	48	225	0.41	11.4	0.11
15-D	α-pinene	52.0	28.0	42.0	12.4	1820	150	53	160	4.52	86.9	0.87
	α-pinene	47.0	28.0	42.0	11.2	no	145	42	180	0.25	5.2	0.05
16-D	α-pinene	186.0	44.0	58.0	32.1	no	180	85	150	4.32	23.2	0.23
	β-pinene	81.0	44.0	58.0	13.9	no	170	68	180	0.12	2.8	0.03
17-D	α-pinene	140.0	37.0	40.0	35.0	no	220	59	147	2.43	19.9	0.20
	β-pinene	227.0	37.0	40.0	56.7	no	210	53		0.06	0.5	0.00
18-D	α-pinene	86.0	60.0	62.0	13.9	no	185	38		0.26	3.5	0.04
	β-pinene	86.5	60.0	62.0	14.0	no	170	16		0.10	6.1	0.06
19-D	α-pinene	144.0	9.0	36.5	39.4	no	120	44	120	10.84	144.5	1.44
	α-pinene	57.0	9.0	36.5	15.6	no	180	35	175	1.30	33.3	0.33
20-D	α-pinene	121.0	61.0	79.0	15.3	2800	125	74	98	5.58	83.3	0.83
	α-pinene	78.0	61.0	79.0	9.9	no	135	66	92	0.14	5.3	0.05
21-D	α-pinene	69.0	42.0	85.0	16.4	no	155	34	175	5.11	96.5	0.96
	β-pinene	65.0	42.0	85.0	15.5	no	170	18		0.01		0.00
22-D	α-pinene	73.0	58.0	94.0	7.8	4300	130	74	140	1.44	30.6	0.31
	α-pinene	73.0	58.0	94.0	7.8	no	140	74	145	0.09	1.5	0.02
23-D	α-pinene	238.0	43.0	98.0	24.3		150	97	160	15.77	66.3	0.66
	isoprene*	208.0					50	113	55, 170	30.77	129.3	1.29
24-D	α-pinene	204.8	95.0	122.0	16.8	750	140	161	185	12.75	66.1	0.66
	isoprene*	97.1					40	208	185	24.34	126.1	1.26

*In addition to α-pinene.

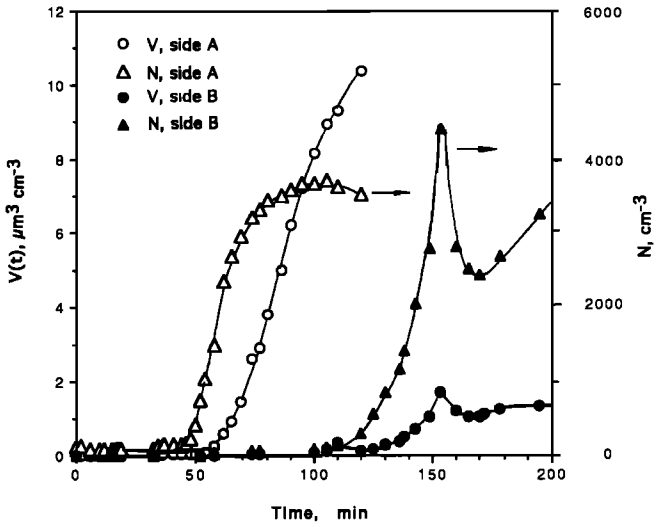

Fig. 2. Aerosol evolution in α-pinene photooxidation in dual-chamber experiment 19D with identical concentrations of NO and NO_x.

min on side A. The volume concentration evidences steady growth. The maximum aerosol volume yield, Y, was 144 μm^3 cm^{-3} ppm^{-1}. On side B, nucleation occurred at 120 min, 70 min later than side A. A second nucleation event occurred at 170 min. The maximum aerosol volume yield on side B was only 33.3 μm^3 cm^{-3} ppm^{-1}.

We understand in principle the general mechanisms by which secondary organic aerosols form in the atmosphere: hydrocarbon photooxidation products of sufficiently low volatility are produced at a sufficient rate that condensation takes place. The lack of knowledge of the detailed reaction mechanisms of the larger hydrocarbons that are likely to be aerosol precursors precludes an a priori calculation of the quantity and molecular nature of secondary aerosol that will result from photooxidation of a particular hydrocarbon.

Oxidizing species in urban air include three electrophiles: ozone (day and night), the hydroxyl radical (OH, daytime only) and the nitrate radical (NO_3, primarily nighttime). The range of reaction rate constants for isoprene, α- and β-pinene with these species is given in Table 2. While it is known that both OH and O_3 are important oxidants of terpenes, the extent of importance of NO_3 under daytime conditions must be estimated. NO_3 radicals are formed from NO and NO_2 by the reaction sequence,

(R1) $NO + O_3 \longrightarrow NO_2 + O_2$

(R2) $NO_2 + O_3 \longrightarrow NO_3 + O_2$

The following reactions remove or temporarily sequester NO_3 radicals,

(R3) $NO_3 + h\nu \longrightarrow NO + O_2$ / $NO_2 + O(^3P)$

(R4) $NO_3 + NO \longrightarrow 2NO_2$

(R5) $NO_3 + NO_2 \longrightarrow N_2O_5$

(R6) $N_2O_5 \longrightarrow NO_3 + NO_2$

TABLE 2. Rate Constants for the OH, O_3, and NO_3 Reactions of Isoprene, α-Pinene, and β-Pinene

Reactant	OH*	O_3†	NO_3‡
Isoprene	1.0×10^{-10}	1.4×10^{-17}	5.9×10^{-13}
α-pinene	5.4×10^{-11}	8.7×10^{-17}	6.2×10^{-12}
β-pinene	7.9×10^{-11}	1.5×10^{-17}	2.5×10^{-12}

Units are cm^3 $molecule^{-1}$ s^{-1}.
Atkinson [1989].
†*Atkinson et. al.* [1990].
‡*Atkinson* [1991].

Because of the rapid consumption reactions, NO_3 concentrations are relatively low under daylight conditions. In addition to the reactions above, NO_3 can also be removed by reaction with organic compounds, such as α- and β-pinene. The rate constants for these six reactions are available [*Atkinson*, 1991]. Thus, NO_3 concentration can be estimated using the pseudosteady state approximation (PSSA),

$$[NO_3] = k_2[NO_2][O_3]/\{k_3 + k_4[NO] + k_7[HC]\} \quad (4)$$

where k_7 (6.2×10^{-12} cm^3 $molecule^{-1}$ s^{-1}) denotes the rate constant of NO_3 with α-pinene at 298K. For the initial conditions of experiment 19D, i.e., α-pinene = 144 ppb, NO = 9 ppb, NO_2 = 25.5 ppb, and O_3 = 20 ppb, NO_3 concentrations estimated with equation (4) are 3.5×10^5 molecule cm^{-3} (1 ppb = 2.46×10^{10} molecule cm^{-3} at 298K and 1 atm). The reaction rate of α-pinene with NO_3 is estimated to be 5% of that with ozone. One concludes that reaction of NO_3 was a minor pathway for consumption of α-pinene in experiment 19D.

The depletion rate of α-pinene can be written as

$$-\frac{d[HC]}{dt} = k_7[HC][NO_3] + k_8[HC][O_3] + k_9[HC][OH] \quad (5)$$

Since the concentrations of α-pinene and ozone were measured during the experiments, and the reaction constants k_8 and k_9 are known (Table 2), the amount of α-pinene reacted with ozone at time t can be determined by numerically integrating,

$$[HC]_{ozone} = \int_0^t k_8[HC][O_3]dt \quad (6)$$

where $k_8 = 8.7 \times 10^{-17}$ cm^3 $molecule^{-1}$ s^{-1}, or 2.14×10^{-6} ppb^{-1} s^{-1}.

Figure 3 shows the total α-pinene that reacted and that portion attributable to the reaction with ozone for experiment 19D-A. The reaction of α-pinene with OH radicals was almost zero initially, and then increased rapidly after OH radical buildup. If we assume that the reactions with ozone and OH radials were the only significant pathways, 62% of the total α-pinene consumption was due to reaction with ozone, and 38% had reacted with OH at 37 min. At 62 min, half of the α-pinene had reacted with ozone and half with OH. At the termination of the experiment, 61.5% of the α-pinene had reacted with ozone and 38.5% had reacted with OH. The OH concentration

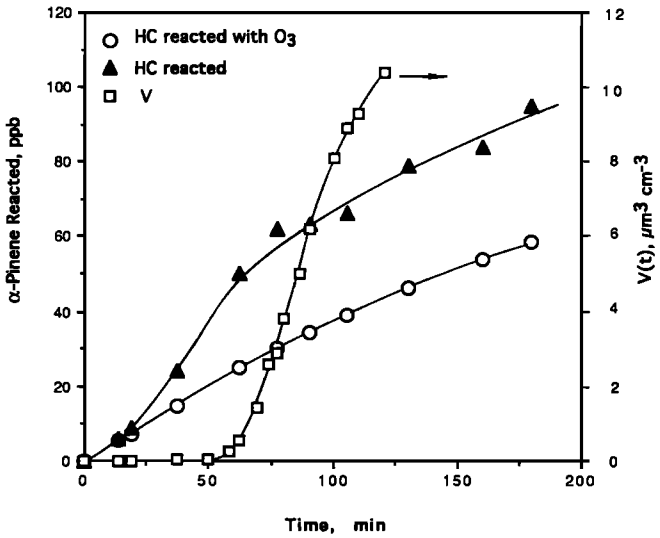

Fig. 3. Total α-pinene that reacted, the α-pinene that reacted with ozone, and total aerosol volume concentration in experiment 19D-A.

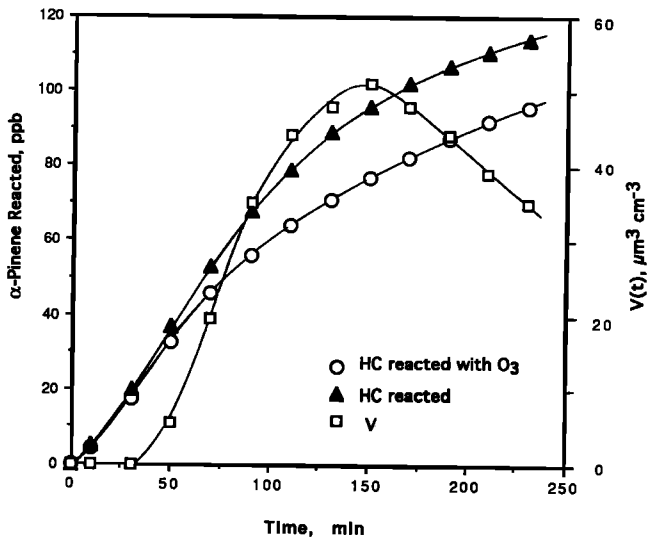

Fig. 5. Total α-pinene that reacted, the α-pinene that reacted with ozone, and total aerosol volume concentration in experiment 13S.

as a function of the reaction time can be calculated using a numerical differentiation method on equation (5), since k_9 is known (k_9 = 5.4 x 10^{-11} cm^3 $molecule^{-1}$ s^{-1}). The time variations of OH, α-pinene reacted, and ozone concentration are shown in Figure 4. The estimated OH radical concentration increased rapidly from almost zero to its maximum, 6.78 x 10^{-5} ppb (16.7 x 10^5 molecules cm^{-3}), in 25 min and then decreased to 1.6 x 10^{-5} ppb. One concludes that both OH and ozone reactions are significant paths to secondary organic aerosol formation with α-pinene.

Experiment 13S exhibited a high aerosol yield. The initial concentration of α-pinene was 158 ppb, and the initial NO_x concentration was 31 ppb. Thus, the ratio $[HC]_o/[NO_x]_o$ was relatively high, 50.8 ppbC/ppb. Nucleation occurred at 35 min of reaction time, and the number concentration N increased from 350 to 22.5 x 10^3 cm^{-3} in 55 min. Condensational growth followed the nucleation almost immediately. The maximum aerosol yield was 514 μm^3 cm^{-3} ppm^{-1} which was achieved at 150 min of reaction time. Concentration profiles similar to those shown in Figures 3 and 4 can be calculated using equations (5) and (6), which are given in Figures 5 and 6. The final percentage of α-pinene that had reacted with ozone was 84.6%, exceeding that in experiment 19D-A. The maximum OH level was estimated to be 7.4 x 10^5 molecules cm^{-3}, lower than that in experiment 19D-A.

Experiment 5S exemplifies low aerosol yield runs. The initial concentration of α-pinene was 188 ppb, but the NO_x concentration was relatively high, 270 ppb. Hence, the ratio $[HC]_o/[NO_x]_o$ was only 6.96 ppbC/ppb. No nucleation was observed during the experiment. Only minor condensation growth of the seed particles occurred after 60 min of reaction

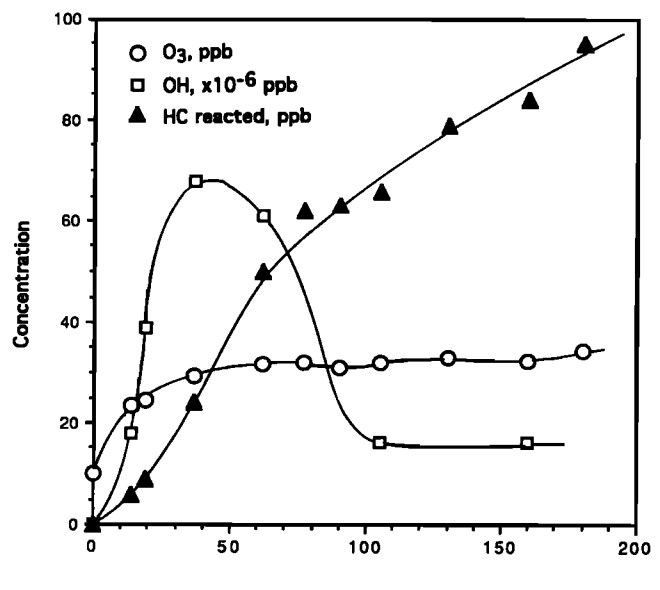

Fig. 4. Concentrations of ozone, OH, and α-pinene that reacted in experiment 19D-A. The concentration of OH was calculated from equation (5).

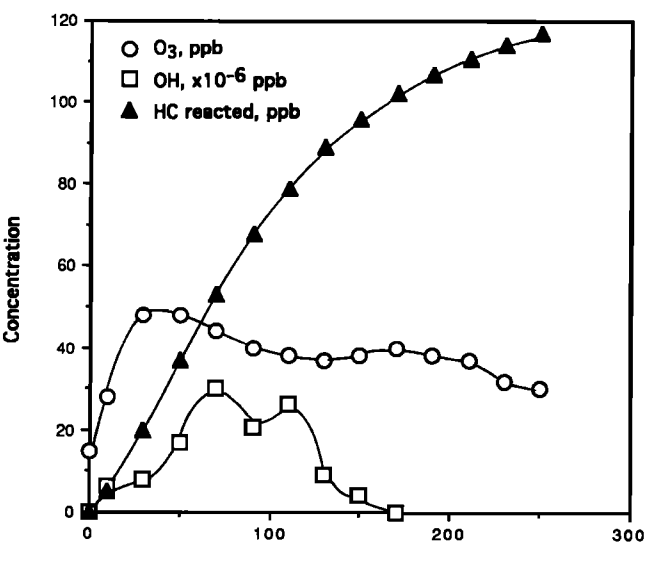

Fig. 6. Concentrations of ozone, OH, and α-pinene that reacted in experiment 13S. The concentration of OH was calculated from equation (5).

time. The maximum aerosol yield was only 8.05 μm^3 cm^{-3} ppm^{-1}.

The maximum aerosol volume concentration V_{max} versus α-pinene reacted for all the experiments is shown in Figure 7. No simple correlation exists between the V_{max} and the α-pinene reacted. However, it should be pointed out that at least 30 ppb of α-pinene was generally consumed before sufficient products accumulated so that the aerosol volume concentration V reached a detectable level, and that V_{max} was a nonlinear function of the α-pinene reacted.

The maximum aerosol volumes V_{max} are shown as a function of the initial concentrations $[HC]_o$ and $[NO_x]_o$ for α-pinene photooxidation in Figure 8. Little or no aerosol formation occurred at relatively low $[HC]_o$ and high $[NO_x]_o$ and a higher V_{max} was obtained at high $[HC]_o$and low $[NO_x]_o$. V_{max} is evidently a strong function of the ratio $[HC]_o/[NO_x]_o$

MAXIMUM AEROSOL YIELD

The maximum aerosol yield is an important quantity for estimating an individual hydrocarbon's contribution to ambient secondary organic aerosol. *Izumi et al.* [1990] pointed out the importance of the ratio, $[HC]_o/[NO_x]_o$ in determining the amount of aerosol produced from aromatic hydrocarbons. However, since they had only one or two data points for each species, they could not correlate the aerosol yield with the $[HC]_o/[NO_x]_o$ ratio. *Pandis et al.* [1991] found the maximum aerosol yield from β-pinene was achieved for a value of $[HC]_o/[NO_x]_o$ in the range of 10 to 20 ppbC/ppb, i.e., 1 to 2 ppb/ppb.

The maximum aerosol volume yield and carbon yield of α-pinene ranged from 0 to 533 μm^3 cm^{-3} ppm^{-1} or 0 to 0.053 for Y_C, and depended strongly on the initial concentrations (see Figure 9). If $[HC]_o/[NO_x]_o$ was less than 10, the aerosol volume yield, Y, was virtually zero. As the ratio increased from 10 to 20, Y increased dramatically. The maximum aerosol volume yield was found to be 533 μm^3 cm^{-3} ppm^{-1} at a ratio of 56. This maximum volume yield is very close to that of β-pinene, 630 μm^3 cm^{-3} ppm^{-1}, found by *Pandis et al.* [1991]. Both studies indicate that aerosol yield depends on the ratio of $[HC]_o/[NO_x]_o$ differing only in the value of the ratio where the yield reaches a maximum.

The aerosol yield is also related to the initial concentration of hydrocarbon. The aerosol yield generally increases as $[HC]_o$ increases and as $[HC]_o/[NO_x]_o$ increases (see Figure 10). A higher concentration of hydrocarbon (α-pinene) leads to a higher aerosol yield since, at low initial hydrocarbon concentration, the concentration of condensable products from photooxidation may not reach the supersaturation level required for nucleation. If the ratio of $[HC]_o/[NO_x]_o$ is fixed, it is likely that lower $[NO]_o$ and higher $[HC]_o$ will give higher aerosol volume yield.

DEPENDENCE OF AEROSOL YIELD ON NO

Hatakeyama et al. [1991] found that the photooxidation of α-pinene and β-pinene with OH in the presence of NO yielded pinonaldehyde and nopinone (6,6-dimethyl-bicyclo(3.1.1) heptan-2one) as major products, respectively. In the absence of NO, the yields of pinonaldehyde and nopinone were substantially lower, and the yield of aerosol increased. A possible reaction sequence of α-pinene with OH and ozone is

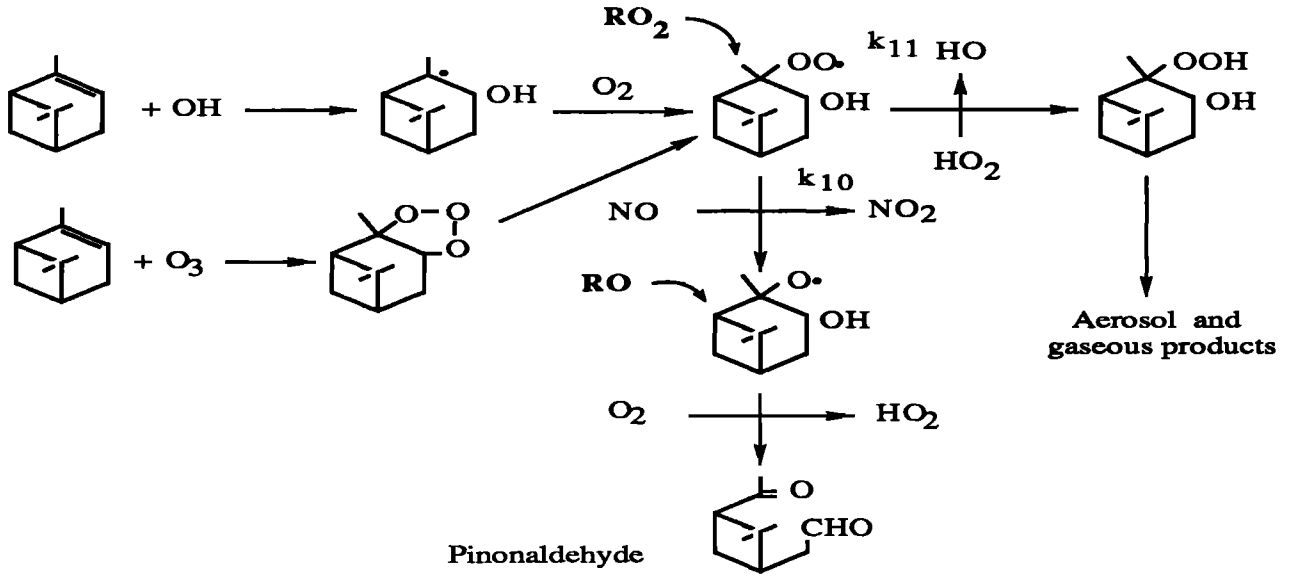

The α-pinene reacts with ozone or with OH and then O_2 to form RO_2 radicals, which have two pathways: (1) RO_2 reacts with NO to yield RO and NO_2, and then RO reacts with O_2 to form pinonaldehyde and HO_2; (2) RO_2 reacts with HO_2 to lead to aerosol and gaseous products. Pinonaldehyde and nopinone will further react with OH to form gaseous products. The β-pinene reactions with OH and ozone in the presence of NO_x are presumed to occur similarly.

While the reaction constants k_{10} and k_{11} have not been measured, estimates can be determined from *Atkinson et al.* [1984] as $k_{10} = 7.6 \times 10^{-12}$ and $k_{11} = 3.0 \times 10^{-12}$ cm^3 $molecule^{-1}$ s^{-1}. Since the constants k_{10} and k_{11} are of the same order of

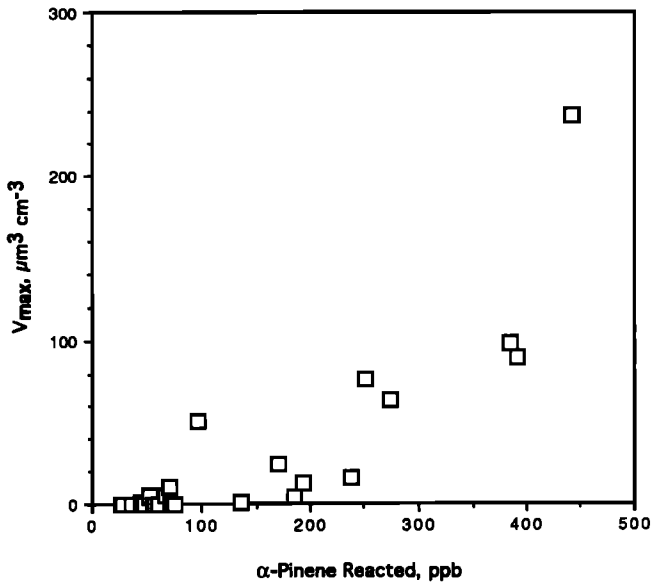

Fig. 7. Maximum aerosol volume concentrations as a function of α-pinene that reacted.

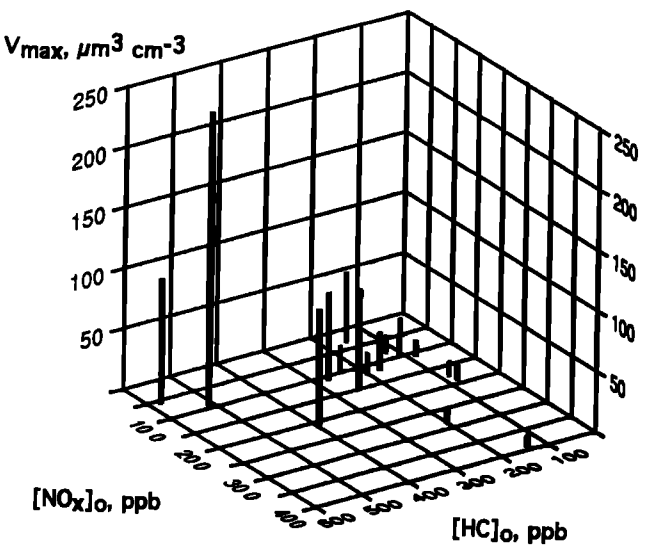

Fig. 8. Aerosol volume concentrations as a function of initial concentrations $[HC]_0$ and $[NO_X]_0$ for α-pinene.

magnitude and the NO concentration in the system is usually much higher than HO_2 at the beginning of photooxidation, most of RO_2 radicals are expected to react with NO to form pinonaldehyde until NO decreases sufficiently.

To estimate the yield of aerosol, the vapor pressure of pinonaldehyde has to be known. Since pinonaldehyde has two oxygen atoms and ten carbon atoms, the vapor pressure of pinonaldehyde should be close to, but not lower than, that of the monocarboxylic acid with the same number of oxygen and carbon atoms. The vapor pressure of the monocarboxylic acid with ten carbon atoms estimated using the correlation from *Grosjean and Seinfeld* [1989] is about 10^{-4} mm Hg, i.e., 130 ppb at ambient temperature. The vapor pressure of pinonaldehyde is likely close to that value. Pinonaldehyde will not form aerosol if its concentration is lower than that level, such as in most of our experiments. However, if the initial concentration of α-pinene is sufficiently high, the concentration of pinonaldehyde can exceed its supersaturation level; thus it can be found in both gaseous and particulate phases [*Hatakeyama et al.*, 1989; *Yokouchi and Ambe*, 1985].

The experimental data of this study can be interpreted based on the above mechanism. Experiments 1S to 5S, except 2S, had low initial ratios $[HC]_0/[NO_x]_0$ (< 7, ppbC/ppb), and low initial concentrations of α-pinene (< 188 ppb) (see Table 1).

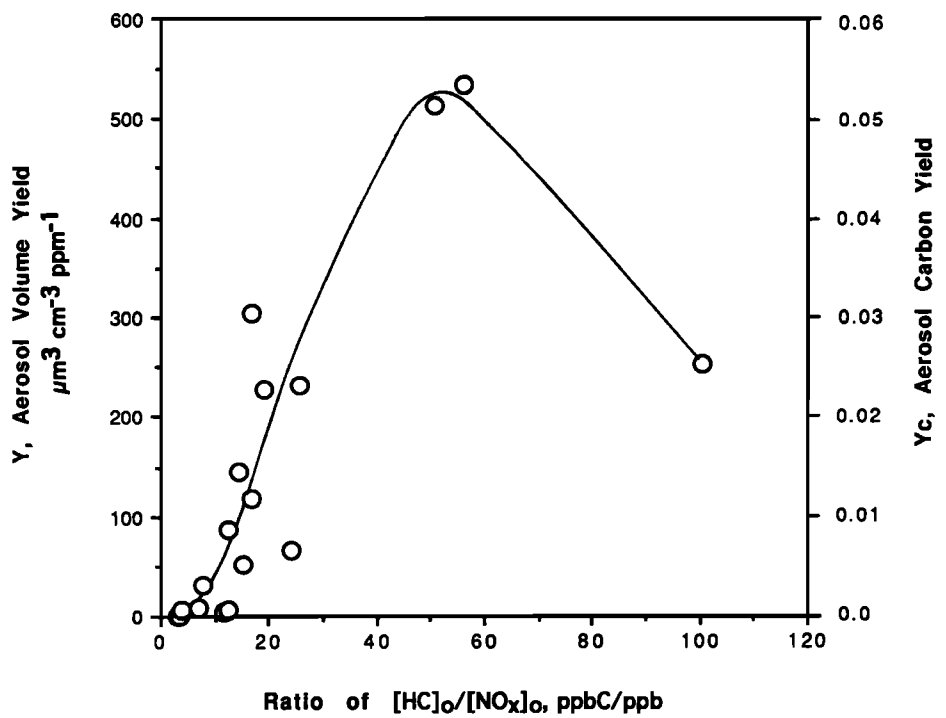

Fig. 9. Maximum Y and Y_C of α-pinene as a function of the ratio $[HC]_0/[NO_X]_0$, (ppbC/ppb).

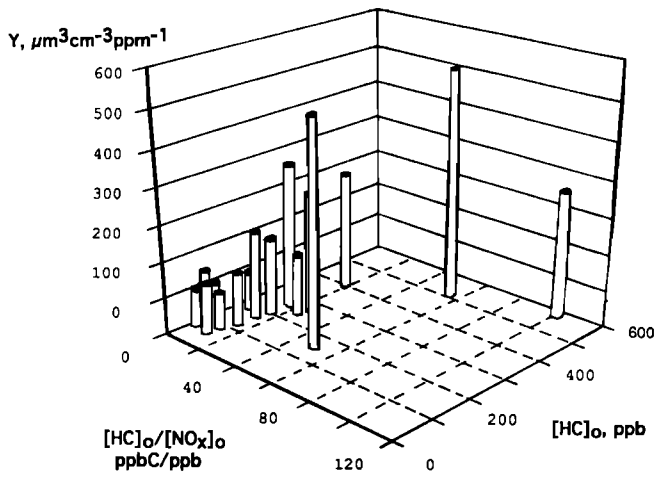

Fig. 10. Maximum aerosol volume yields of α-pinene as a function of the ratio $[HC]_o/[NO_x]_o$ and $[HC]_o$.

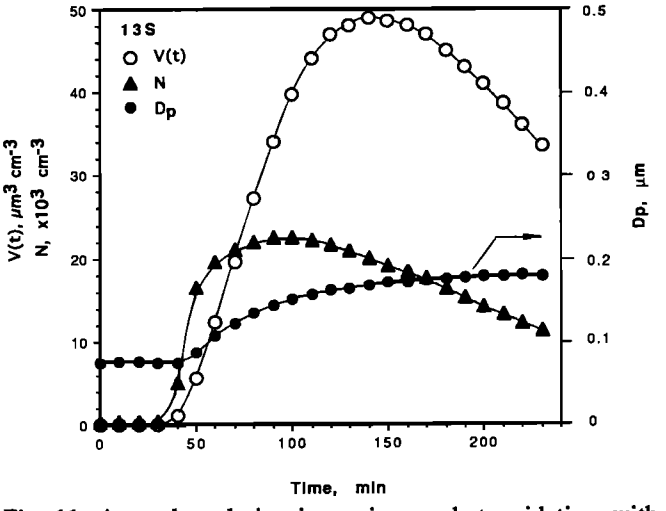

Fig. 11. Aerosol evolution in α-pinene photooxidation with seed particles in experiment 13S.

The initial molar ratios of [HC] to $[NO_x]$ for experiments 1S, 3S, 4S, and 5S are less than 1, which means that pinonaldehyde was likely one of the major primary photooxidation products. Since the initial concentrations of α-pinene in these experiments were less than 188 ppb and yields of pinonaldehyde from the α-pinene/OH and α-pinene/O_3 reactions were reported to be 0.56 and 0.51, respectively [*Hatakeyama et al.*, 1989, 1991], pinonaldehyde could reach a maximum concentration of only 105 ppb, which is below the estimated supersaturation level. Therefore, virtually no aerosol was formed in those experiments. With high initial ratios $[HC]_o/[NO_x]_o$ (15 to 100, ppbC/ppb) and higher initial concentrations of α-pinene (160 to 582 ppb), such as in experiments 7S to 13S, the molar ratio of $[HC]_o$ to $[NO_x]_o$ ranged from 1.5 to 10, both OH and O_3 reaction pathways were likely significant. Although the extent of importance of RO_2 - HO_2 path is unknown, to the extent that it occurred, it is presumed to lead both aerosol and gaseous products. Thus, the higher ratios $[HC]_o/[NO_x]_o$ and higher hydrocarbon concentrations lead to a higher aerosol yield.

THE EFFECT OF SEED PARTICLES

In a number of the experiments, ammonium sulfate particles were introduced into the smog chamber. The number concentration N of seed particles varied from 180 to 4000 cm^{-3}, however for most runs, the number concentrations did not exceed 1000 cm^{-3}. Seed particles provide condensation sites for supersaturated condensable photooxidation products. If gas-to-particle conversion by condensation rates is lower than the rates of generation of condensable products, supersaturation increases and nucleation can occur. Both aerosol number and volume concentrations increased (see Figure 11). By contrast, if the initial number concentration of seed particles was in the range of 1000-4000 cm^{-3}, and the generation rate of condensable products was relatively low, only condensation occurred.

Dual-chamber experiment 15D was carried out with the same concentrations of NO and NO_x on each side; 28, 42 ppb, respectively, and almost the same hydrocarbon concentration on both sides, 52 and 47 ppb of α-pinene. The ratio $[HC]_o/[NO_x]_o$ is approximately 12 ppbC/ppb. However, there were seed particles at a concentration of 2100 cm^{-3} as an initial concentration on side A, and no no initial aerosol on side B. The aerosol evolution on side A is shown in Figure 12. During the first 50 min, the number concentration of particles, primarily the seed particles, on side A gradually decreased from 2100 cm^{-3} to 1850 cm^{-3}, as a result of wall deposition. Then both number concentration N and aerosol volume concentration V started to increase. N reached its maximum of 2600 cm^{-3} at 125 min of reaction time, and V reached its maximum value of 4.52 $\mu m^3\ cm^{-3}$ at 160 min. Under this experimental condition the primary particles provided most, but not all, of the surface area for condensation. The maximum aerosol volume yield was 86.9 $\mu m^3\ cm^{-3}\ ppm^{-1}$. On side B, without seed particles, some nucleation and growth occurred. N increased from 50 to 200 cm^{-3} and aerosol volume yield was only 5.23 $\mu m^3\ cm^{-3}\ ppm^{-1}$.

In dual-chamber experiment 22D, with the same initial concentrations of α-pinene, NO, and NO_x on both sides, there were seed particles on side A, at a concentration of 4300 cm^{-3}, and no seed particles on side B. With a relatively low ratio $[HC]_o/[NO_x]_o$ of 7.7, no nucleation or condensation occurred on either side.

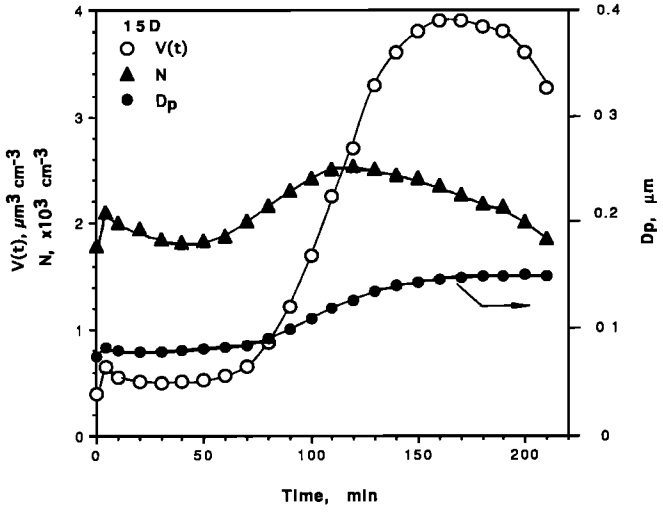

Fig. 12. Aerosol evolution in α-pinene photooxidation with seed particles in experiment 15D.

Although the effect of seed particles on the number concentration of aerosol particles is significant in α-pinene/NO_x photooxidation, the effect on the ultimate aerosol yield is minor. The aerosol yield for α-pinene/NO_x photooxidation depends mainly on the initial concentrations of HC and NO_x as discussed earlier. Nevertheless, seed particles can provide sites for aerosol growth and therefore reduce the threshold for condensation. It was observed during the α-pinene/NO_x photooxidation with seed particles, such as experiments 13S and 15D, that condensation started as soon as 20 ppb of α-pinene had reacted. Without seed particles, nucleation occurred when as little as 35-40 ppb of α-pinene had reacted. As expected, a somewhat higher supersaturation is needed for nucleation than for condensation.

COMPARISON OF α-PINENE AND β-PINENE

The study of *Pandis et al.* [1991] on β-pinene photooxidation found similar maximum aerosol yields to those for α-pinene determined in this study. However, it is informative to compare the photooxidation kinetics of the two species in dual-chamber experiments. Four dual-chamber experiments with different initial concentration ratios were carried out and are listed in Table 3.

In dual-chamber experiment 18D, initial α- and β-pinene, NO, and NO_x concentrations were the same on both sides, $[HC]_o/[NO_x]_o$=13.9. No nucleation or condensation was observed. The high initial concentration of NO (96% of NO_x) suppressed the aerosol formation, which is consistent with the results from earlier experiments. The concentration variations with time of that experiment are shown in Figure 13. The α-pinene was more quickly photooxidized than β-pinene and gave a higher yield of ozone over the time period of the experiment.

Identical concentrations of NO and NO_x, but different concentrations of α-pinene and β-pinene, were employed in experiments 16D and 17D. The photooxidation of α-pinene was faster than β-pinene as it was in experiment 18D. On the α-pinene side, nucleation and condensational growth occurred at 60 min and the aerosol number concentration, N, reached 1500 cm^{-3} at 75 min. On the β-pinene side, only a small amount of nucleation was observed at 140 min. The aerosol volume yield of α-pinene photooxidation was also considerably higher than that from β-pinene.

The α-pinene-OH rate constant is 32% lower than that of β-pinene, but the rate constant of α-pinene with ozone is 5.4 times higher than that of β-pinene (Table 2). Because of these rate constant differences, the depletion rate of α-pinene, $\{-d[\alpha\text{-pinene}]/dt\}_{max}$, is about six times of that of β-pinene, $\{-d[\beta\text{-pinene}]/dt\}_{max}$ in experiment 18D (Figure 13). Because of the relatively low reaction rate constant of β-pinene with ozone, the reaction of β-pinene with ozone played a minor role until significant ozone buildup, and OH consumed most of the β-pinene. The ozone buildup process required 3 to 6 hours to reach the maximum in the β-pinene/NO_x photooxidation experiments [*Pandis et al.*, 1991], while a majority of the α-pinene studied here reacted earlier with ozone because of its higher rate constant.

The tentative conclusion can be drawn is that at concentrations of NO_x, α-pinene or β-pinene less than 100 ppb, typical of ambient conditions, α-pinene is photooxidized faster than β-pinene at the same concentrations of NO and NO_x, and produces higher ozone and aerosol yields over a

TABLE 3. Comparison of Aerosol Formation From α- and β-Pinene

Run	Hydrocarbon	Initial Concentrations			$[HC]_o/[NO_x]_o$	Seeds,	Ozone, Maximum		V_{max}	Y,	Y_c,
		HC, ppb	NO, ppb	NO_x, ppb	ppb C/ppb	cm^{-3}	Time, min	ppb	$\mu m^3\ cm^{-3}$	$\mu m^3\ cm^{-3}\ ppm^{-1}$	%
16-D	α-pinene	186.0	44.0	58.0	32.1	no	180	85	4.32	23.2	0.23
	β-pinene	81.0	44.0	58.0	13.9	no	170	68	0.12	2.8	0.03
17-D	α-pinene	140.0	37.0	40.0	35.0	no	220	59	2.43	19.9	0.20
	β-pinene	227.0	37.0	40.0	56.7	no	210	53	0.06	0.5	0.00
18-D	α-pinene	86.0	60.0	62.0	13.9	no	185	38	0.26	3.5	0.04
	β-pinene	86.5	60.0	62.0	13.9	no	170	16	0.10	6.1	0.06
21-D	α-pinene	69.0	42.0	85.0	16.4	no	155	34	5.11	96.5	0.96
	β-pinene	65.0	42.0	85.0	15.5	no	170	18	0.01	0.0	0.00
23-D	α-pinene	238.0	43.0	98.0	24.3		150	97	15.8	66	0.66
	isoprene*	208.0			24.3		50	113	30.8	129	1.29
24-D	α-pinene	204.8	95.0	122.0	16.8	750	140	161	12.8	66	0.66
	isoprene*	97.1			16.8		140	208	24.3	126	1.26
12-S	α-pinene and isoprene	370.0 613.3	12.0	35.8	103.4	400	40	58	150.3	995	9.93

*In addition to α-pinene, and $[HC]_o/[NO_x]_o$ is evaluated for α-pinene only.

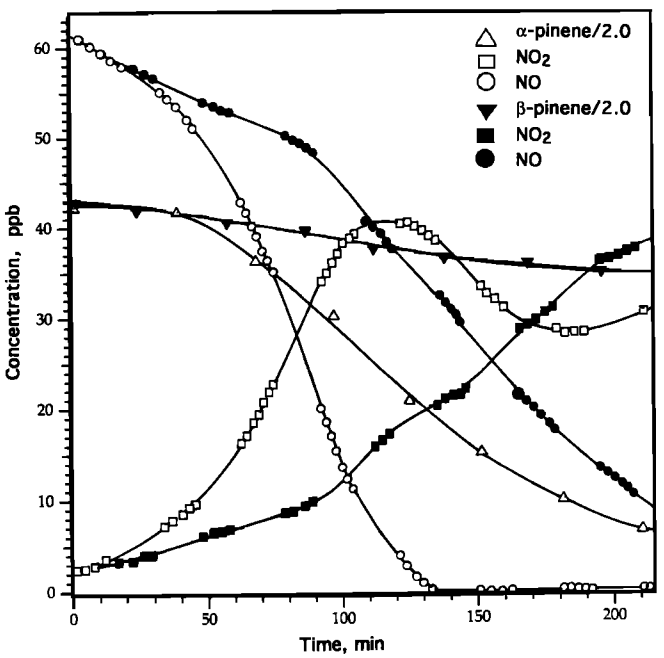

Fig. 13. The α-pinene and β-pinene that reacted with NO_x in dual-chamber experiment 18D. The open symbols represent α-pinene side and the solid symbols represent β-pinene side.

given period of time. However, since these dual-chamber experiments were carried out over only about 3 hours, and only half of the β-pinene was reacted, it is expected based on the observations of *Pandis et al.* [1991] that the aerosol yield of β-pinene would continue to increase with sufficiently long reaction time.

EFFECT OF ISOPRENE ON AEROSOL YIELD OF α-PINENE

The aerosol yield from isoprene photooxidation at ambient concentration levels as reported by *Pandis et al.* [1991] is negligible. Nevertheless, the presence of isoprene may have some effect on the aerosol formation of other hydrocarbons present through the enhanced photochemical activity provided by isoprene.

One dual-chamber experiment 24D was designed with identical concentrations of α-pinene (204.8 ppb), NO and NO_x (95, 122 ppb) on both sides. The ratio of $[HC]_o/[NO_x]_o$ was 16.8 ppbC/ppb. An initial amount isoprene, 97.1 ppb, was injected into side A only. The resulting hydrocarbon and ozone concentrations are shown in Figure 14. The α-pinene on side A was photooxidized faster in the presence of isoprene, the maximum ozone concentration achieved was 27% higher on side A. The comparison of aerosol evolution is given in Table 3. On side A, with isoprene, some condensation occurred at 100 min, then nucleation occurred at 130 min, the number concentration increased to 6600 cm^{-3} at 160 min. On side B, condensation started at about 100 min, and no nucleation was observed. The maximum aerosol volume concentrations were 24.3 $\mu m^3\ cm^{-3}$ and 12.7 $\mu m^3\ cm^{-3}$ for sides A and B, respectively.

Based on the results of *Pandis et al.* [1991] no aerosol would form even if all 97.1 ppb of isoprene had reacted. Hence, all the secondary aerosol formed was a result of α-pinene photooxidation. Thus, the aerosol carbon yield, 1.26%, on side A was twice that of side B. Similarly, 152 ppb of isoprene and 151 ppb of α-pinene were photooxidized in experiment 12S. The Y_c of 9.94% is also approximately twice that of 5.3% in experiment 11S in the absence of isoprene.

It was observed in experiment 24D that NO decreased from 95 ppb to a few ppb and ozone increased from 15 to 180 ppb in 70 min. The ozone concentration reached 208 ppb. In contrast, in the absence of isoprene on side B, the ozone concentration reached only 161 ppb. The presence of isoprene obviously increased photochemical activity, one result of which is a higher aerosol yield from the α-pinene present.

ATMOSPHERIC IMPLICATIONS

The annual emissions of isoprene and monoterpenes have been estimated at 30.7 Mt in the United States, which exceeds the national anthropogenic volatile organic carbon emission estimate of 18.2 Mt yr^{-1} [*Lamb et al.*, 1987]. The concentration of isoprene has been found to range from near zero at night to levels in excess of 30 ppb during daylight hours in a deciduous forest [*Martin et al.*, 1991]. The concentrations of monoterpenes in coniferous forests range from tenths of a ppb in daytime to several ppb at night [*Janson*, 1992]. Since the concentration of NO in the clean troposphere generally does not exceed 0.05 ppb, and the concentration of NO_2 is less than 0.5 ppb, the hydrocarbon-to-NO_x ratio is high. Thus, the suppression of aerosol yield by NO will not hold, and it is reasonable to make estimates of terpene aerosol yields based on the upper values determined in this study.

Assuming the density of aerosol product from the photooxidation of α- and β–pinene is 1.0 pg μm^{-3}, we can convert a 5.3% aerosol carbon yield to a 10.8% aerosol mass yield (using C = 1.0 instead of 0.49 in equation 2). Thus, 2.7

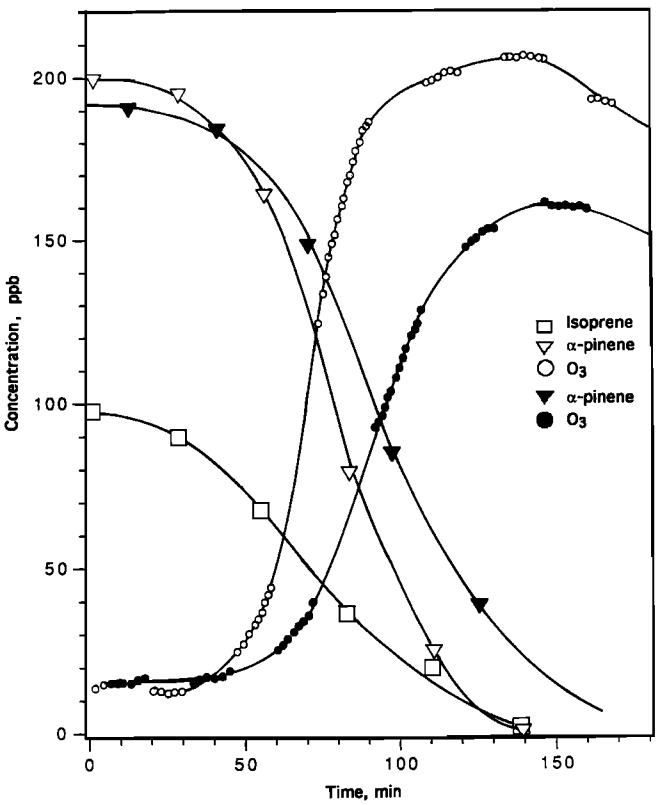

Fig. 14. Effect of isoprene on α-pinene photooxidation in dual-chamber experiment 24D. The open symbols represent the α-pinene side with isoprene.

Mt aerosol is estimated to result annually from photooxidation of 24.8 Mt of monoterpenes. If we assume that the amount of aerosol is distributed evenly over the continental United States, we estimate 338 kg km^{-2} yr^{-1} of aerosol, i.e., 0.926 kg km^{-2} d^{-1}, or 0.454 kg C km^{-2} d^{-1}. We can compare this estimated biogenic aerosol production rate with the anthropogenic rate of emissions of fine aerosol carbon. The fine aerosol carbon emissions in the central portion of the South Coast Air Basin of California have been estimated to be 39 x 10^3 kg C d^{-1} in an 80 x 80 km^2 area in 1982 [*Gray*, 1986], i.e., 6.1 kg C km^{-2} d^{-1} This emission rate of anthropogenic aerosol carbon in probably the most polluted region of the United States is 13 times that of the estimated continental average biogenic aerosol carbon emission rate. Since more than half of the biogenic hydrocarbon emissions are estimated to occur in the summer, and approximately half are estimated to arise in the southeast and southwest United States, more concentrated biogenic aerosols are expected in these areas and in the summer season.

CONCLUSIONS

Aerosol formation and growth in α-pinene/NO_x and β-pinene/NO_x photooxidation have been studied in an outdoor smog chamber. The reactant concentrations ranged from a few ppb to several hundred ppb. The aerosol carbon yield in α-pinene/NO_x photooxidations ranged from zero to 5.3% for α-pinene concentrations between 30 and 580 ppb, the value of which is highly dependent on the initial concentration ratio $[HC]_o/[NO_X]_o$. If the ratio $[HC]_o/[NO_X]_o$ was less than 10 ppbC/ppb, little nucleation or growth was observed. The aerosol yield increased dramatically as the ratio increased from 10 to 20. The maximum aerosol yield was observed at a ratio of 56. The nucleation threshold is around 35 ppb of α-pinene reacted, and the condensation threshold is below 20 ppb of α-pinene reacted. The α-pinene/O_3 and α-pinene/OH reactions are the major pathways.

The photooxidation rate of α-pinene was about six times that of β-pinene under the same conditions, hence α-pinene/NO_x photooxidation will have higher yields of ozone and aerosol in a given period of time. However, with sufficiently long reaction times the ultimate aerosol yield of β-pinene is expected to be close to that of α-pinene. Although isoprene/NO_x photooxidation does not contribute directly to the production of secondary aerosol under ambient conditions, the co-existence of isoprene and α-pinene increases the aerosol yield from α-pinene/NO_x photooxidation substantially. An aerosol carbon yield as high as 10% was obtained based on the α-pinene consumption in the presence of isoprene.

Based on the data obtained in this study and in previous work, biogenic hydrocarbons have potential to contribute significantly to secondary organic aerosol formation especially in regions with sufficient vegetation.

Acknowledgments. This work was supported by the Coordinating Research Council, project AQ-3-2, and National Science Foundation grant ATM-9003186.

REFERENCES

Atkinson, R., Kinetics and mechanisms of the gas-phase reactions of the hydroxyl radical with organic compounds, *J. Phys. Chem. Ref. Data, Monogr. 1*, 111-112, 1989.

Atkinson, R., Kinetics and mechanisms of the gas-phase reactions of the NO_3 radical with organic compounds, *J. Phys. Chem. Ref. Data, 20*, 459-507, 1991.

Atkinson, R., and A.C. Lloyd, Evaluation of kinetic and mechanistic data for modeling of photochemical smog, *J. Phys. Chem. Ref. Data, 13*, 315-444, 1984.

Atkinson, R., D. Hasegawa , and S.M. Aschmann, Rate constants for the gas-phase reactions of O_3 with a series of monoterpenes and related compounds at 296 ± 2 K, *Int. J. Chem. Kinet., 22*, 871-887, 1990.

Dimitriades, B., The role of natural organics in photochemical air pollution: issues and research needs, *J. Air Pollut. Control Assoc., 31*, 229-235, 1981.

Gray, H.A., Control of atmospheric fine primary carbon particle concentrations, Ph D. thesis, California Institute of Technology, Pasadena, 1986.

Grosjean, D., and J.H. Seinfeld, Parameterization of the formation potential of secondary organic aerosols, *Atmos. Environ., 23*, 1733-1744, 1989.

Hatakeyama, S., K. Izumi, T. Fukuyama, and H. Akimoto, Reaction of ozone with α-pinene and β-pinene in air: Yields of gaseous and particulate products, *J. Geophys. Res., 94*, 13013-13024, 1989.

Hatakeyama, S., K. Izumi, T. Fukuyama, H. Akimoto, and N. Washida, Reactions of OH with α-pinene and β-pinene in air: estimate of global CO production from the atmospheric oxidation of terpenes, *J. Geophys. Res., 96*(D1), 947-958, 1991.

Hering, S.V., R.C. Flagan, and S.K. Friedlander, Design and evaluation of a new low-pressure impactor, 1, *Environ. Sci. Technol., 12*, 667-673, 1978.

Hering, S.V., S.K. Friedlander, J.J.Collins, and L.W. Richards, Design and evaluation of a new low-pressure impactor, 2, *Environ. Sci. Technol., 13*, 184-188, 1979.

Hooker, C.L., and H.H. Westberg, Determination of carbon balances for smog chamber terpene oxidation experiments using a ^{14}C tracer technique, *J. Atmos. Chem., 2*, 307-320, 1985.

Hull, L.A., Terpene ozonolysis products, in *Atmospheric Biogenic Hydrocarbons, vol. 2*, edited by J.J. Bufalini and R.R. Arnts , pp. 161-186, Butterworth, Stoneham, Mass., 1981.

Izumi, K., and T. Fukuyama, Photochemical aerosol formation from aromatic hydrocarbons in the presence of NO_X, *Atmos. Environ., Part A, 24*, 1433-1441, 1990.

Izumi, K., K. Murano, M. Mizuochi, and T. Fukuyama, Aerosol formation by the photooxidation of cyclohexene in the presence of nitrogen oxides, *Environ. Sci. Technol., 22*, 1207-1215, 1988.

Janson, R., Monoterpene concentrations in and above a forest of scots pine, *J. Atmos. Chem., 14*, 385-394, 1992.

Kamens, R.M., H.E. Jeffries, M.W. Gery, R.W. Wiener, K.G. Sexton, and G.B. Howe, The impact of alpha-pinene on urban smog formation: An outdoor smog chamber study, *Atmos. Environ., 15*, 968-981, 1981.

Lamb, B., A. Guenther, D. Gay, and A. Westberg, A national inventory of biogenic hydrocarbon emissions, *Atmos. Environ., 21*, 1695-1705, 1987.

Liu, B.Y., and K.W. Lee, An aerosol generator of high stability, *Am. Ind. Hyg. Assoc. J., 36*, 861- 865, 1975.

Martin, R.S., H. Westberg, E. Allwine, L. Ashman, J.C. Farmer, and B. Lamb, Measurement of isoprene and its atmospheric oxidation products in a central Pennsylvania deciduous forest, *J. Atmos. Chem., 13*, 1-32, 1991.

Pandis, S.N., S.E. Paulson, J.H. Seinfeld, and R.C. Flagan, Aerosol formation in the photo-oxidation of isoprene and

β-pinene, *Atmos. Environ., Part A, 25,* 997-1008, 1991.

Paulson, S.E., S.N. Pandis, U. Baltensperger, J.H. Seinfeld, R.C. Flagan, E.J. Palen, D.T. Allen, C. Schaffner, W. Giger, and A. Protmann, Characterization of photochemical aerosols from biogenic hydrocarbons, *J. Aerosol Sci., 21,* 245-248, 1990.

Wang, S.C. and R.C. Flagan, Scanning electrical mobility spectrometer, *Aerosol Sci. Technol., 13,* 230-240, 1990.

Went, F.W., Blue hazes in the atmosphere, *Nature, 187,* 641-643, 1960.

Yokouchi, J., and Y. Ambe, Aerosols formed from the chemical reaction of monoterpenes and ozone, *Atmos. Environ., 19,* 1271-1276, 1985.

R.C. Flagan, J.H. Seinfeld, M. Shaw, and S.H. Zhang, Department of Chemical Engineering, California Institute of Technology, Pasadena, CA 91125.

(Received June 1, 1992;
revised August 21, 1992;
accepted September 1, 1992.)